Smart Structures and Systems, *Vol. 29, No. 3 (2022) 445-455*
https://doi.org/10.12989/sss.2022.29.3.445

Modeling and optimization of infill material properties of post-installed steel anchor bolt embedded in concrete subjected to impact loading

Muhammad Saleem*

Department of Mechanical and Energy Engineering, College of Engineering, Imam Abdulrahman Bin Faisal University, P.O. Box 1982, Dammam 31441, Eastern Province, Kingdom of Saudi Arabia

(*Received January 4, 2021, Revised December 4, 2021, Accepted December 7, 2021*)

Abstract. Steel anchor bolts are installed in concrete using a variety of methods. One of the most common methods of anchor bolt installation is using epoxy resin as an infill material injected into the drilled hole to act as a bonding material between the steel bolt and the surrounding concrete. Typical design standards assume uniform stress distribution along the length of the anchor bolt accompanied with single crack leading to pull-out failure. Experimental evidence has shown that the steel anchor bolts fail owing to the multiple failure patterns, hence these design assumptions are not realistic. In this regard, the presented research work details the analytical model that takes into consideration multiple micro cracks in the infill material induced via impact loading. The impact loading from the Schmidt hammer is used to evaluate the bond condition bond condition of anchor bolt and the epoxy material. The added advantage of the presented analytical model is that it is able to take into account the various type of end conditions of the anchor bolts such as bent or U-shaped anchors. Through sensitivity analysis the optimum stiffness and shear strength properties of the epoxy infill material is achieved, which have shown to achieve lower displacement coupled with reduced damage to the surrounding concrete. The accuracy of the presented model is confirmed by comparing the simulated deformational responses with the experimental evidence. From the comparison it was found that the model was successful in simulating the experimental results. The proposed model can be adopted by professionals interested in predicting and controlling the deformational response of anchor bolts.

Keywords: concrete; epoxy; experimental validation; grout; impact loading; material properties; micro-cracking model; non-destructive test; pull-out response; shear strength; steel anchor bolt; stiffness

1. Introduction

Anchor bolts have large variety of applications in various industries such as construction, mining, mechanical etc. Their usefulness ranges from installing signposts, lights to fixing permanent structures. Steel anchor bolts are also used for adding extensions to existing structures. Currently much research work is being focused on steel anchor bolts for their increased application in prefabricated structural elements. Eligehausen and Balogh (1995), Eligehausen *et al*. (2006) and Mallee *et al*. (2013) presented the in-depth design guidelines for engineers and researchers related to anchor bolts installed in concrete post-construction. The researchers took into consideration monotonic and cyclic loading, fatigue and design limit state for proposing the anchor bolt system design guidelines. Takiguchi *et al*. (1999) and Zamora *et al*. (2003) also investigated the deformational response of various types of grouted, headed and straight anchor bolts. Lê Minh *et al*. (2012), Ceci *et al*. (2012), and Ouyang *et al*. (1994) presented crack development and propagation models for steel fibers reinforced concrete. The researchers also conducted beam strengthening experiments using fiber reinforced concrete and reported improvement in deformational response of structural elements owing to the anchoring effect of steel fibers which was deemed similar to anchors embedded in concrete. Guillet (2011) and Hoehler and Eligehausen (2008a, b) reported through their experimental work that the bond between embedded steel anchor bars deteriorated owing to micro-cracking at the interface of steel and concrete. Philipp *et al*. (2016) and Saleem (2018a, b, c) presented the analytical model related to the multiple crack extension of anchor bolts embedded in concrete using both monotonic and cyclic loading. The researchers presented models with capable of predicting experimental results and real-world deformational response.

In the past much effort by the researchers was exerted on the developing bond evaluation models and experimental evidence. However, little to no attention was paid on developing a non-destructive testing method that can be reliably employed to estimate the pull-out strength and bond performance of anchor bolts and steel anchor bars. In this regard Saleem and Nasir (2016), Saleem *et al*. (2016), Saleem and Hosoda (2017), Saleem (2020), Saleem and Almakhayitah (2020), Saleem and Hector (2021), Saleem and Hosoda (2021), developed a novel non-destructive testing method to evaluate the pull-out strength of anchor bolts embedded in the concrete. The researchers also developed a method to identify and isolate the internal cracking in the structural elements. The proposed testing

*Corresponding author, Ph.D., Associate Professor,
E-mail: mssharif@iau.edu.sa

ISSN: 1738-1584 (Print), 1738-1991 (Online)

methods has been employed in real-world for structural health evaluation and bond quality assessment of reinforced concrete structures. ACI 349-13 and ACI 318-14 design codes categorize the failure of the steel anchor bolts into four types: (a) bolt rupture; (b) cone failure; (c) pull-out failure; and (d) splitting rupture. Cone type of failure is most commonly reported in the literature and also observed in real-world conditions (Yang and Ashour 2009, Caggiano and Martinelli 2012, Chen 2014). However, the influence of the grout material also plays a critical role in the pull-out performance of the anchor bolt as reported by Barani and Khoei (2014).

Through the presented detailed literature review it is evident that much research work in the past has been focused on the understanding the deformational response of anchor bolts under cyclic and monotonic loading. Also, efforts by the researchers have been focused on developing NDT for evaluating the strength of anchor bolts and bars. However, very little effort has been spent on understanding the effect of grout/epoxy material properties on the deformational response of steel anchor bolts installed post-construction. The presented analytical model takes into consideration the all mechanical and material factors that affect the pull-out performance of steel anchor bolts such as diameter, embedment length, concrete quality, bond strength, grout/epoxy material properties and anchor bolt end condition i.e., L-type hook, U-type hook or unheeded straight anchors. Lastly, an optimized set of material properties for the grout/epoxy is presented along with validating the model by comparing its deformational response with the experimental results. The presented set of optimized material properties and the proposed analytical model can be used by professional interested in predicting and controlling the deformational response of anchor bolts installed using epoxy injection.

2. Materials and methods

2.1 Materials

Sixty 300 × 300 × 300 mm concrete cube specimens we cast along with twelve 150 × 300 mm cylindrical specimens for compressive strength evaluation. OPC type-1 with specific gravity of 3.14 was used for casting of the samples in accordance with ASTM C150. The rational for choosing OPC type-1 was based on the logic that it is most widely adopted material used in a variety of industrial applications, hence any research and development using this type of cement will have the largest real-world application. Hence, the choice of using OPC type-1 had logical rational background. Desert sand was used as a source of fine aggregate with the water absorption ratio and specific capacity of 0.71% and 2.55 respectively. The water-to-cement ration was kept at 0.39 with water equal to 123 kg/m^3; cement 270 kg/m^3, air entrainment 3.9%; sand and gravel 819 and 1011 kg/m^3, respectively. Limestone was used as a coarse aggregate with a maximum size of 18 mm graded according to the specification of ASTM C33. The coarse aggregate consisted of water absorption percentage and bulk specific gravity of 1.95% and 2.41, respectively. A Slump of 100 $\pm$ 25 mm was recorded, and the samples were cured in a temperature-controlled lab with the average compressive strength of 33.4 MPa recorded after 28 days of curing.

2.2 Methods

Steel anchor bolts typically used for small to medium application in the construction industry were used in the experimental investigation. The anchor bolts were installed in pre-drilled holes using epoxy resin in accordance with the ASTM C881. The total length of the stainless-steel anchor bolt, L_C was 150 mm. 70 mm and 50 mm was embedded into the pre-drilled holes referred to as, L_E, while the remaining was outside the hole, referred to as exposed length, L_O as shown in Fig. 1. Each bolt was tested for hardness using the Rockwell hardness test with hardness number of B70. Immense care was taken in aligning the bolt in the middle of the pre-drilled hole. Five rebound readings using Schmidt hammer were induced on the top of the anchor bolt as depicted in the Fig. 1. The experimental details pertaining to casting, curing and experimentation, data collection, analysis and results of Schmidt hammer testing can be found on earlier published work by the research group (see Saleem and Nasir 2016, Saleem *et al*. 2016, Saleem 2017, 2020, Saleem and Almakhayitah 2020, Saleem and Hector 2021, Saleem and Hosoda 2021). The objective of the presented research work is to focus on the experimental validation and infill material properties optimization to achieve desired pull-out strength for various types of steel anchor bolts. Previously, Saleem *et al*. (2016),

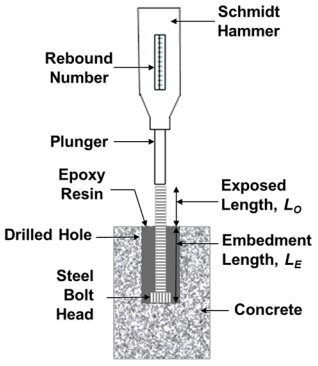

Fig. 1 Rebound reading testing setup

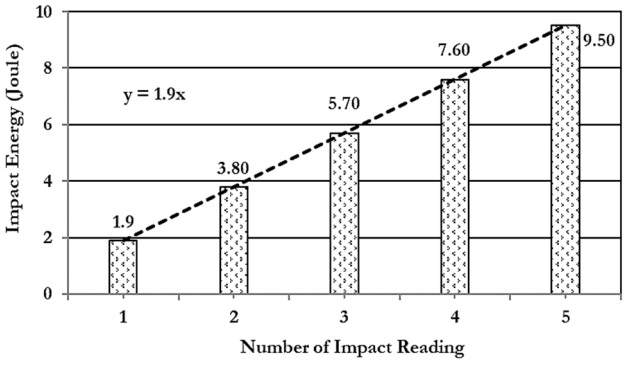

Fig. 2 Impact energy induced onto anchor bolt

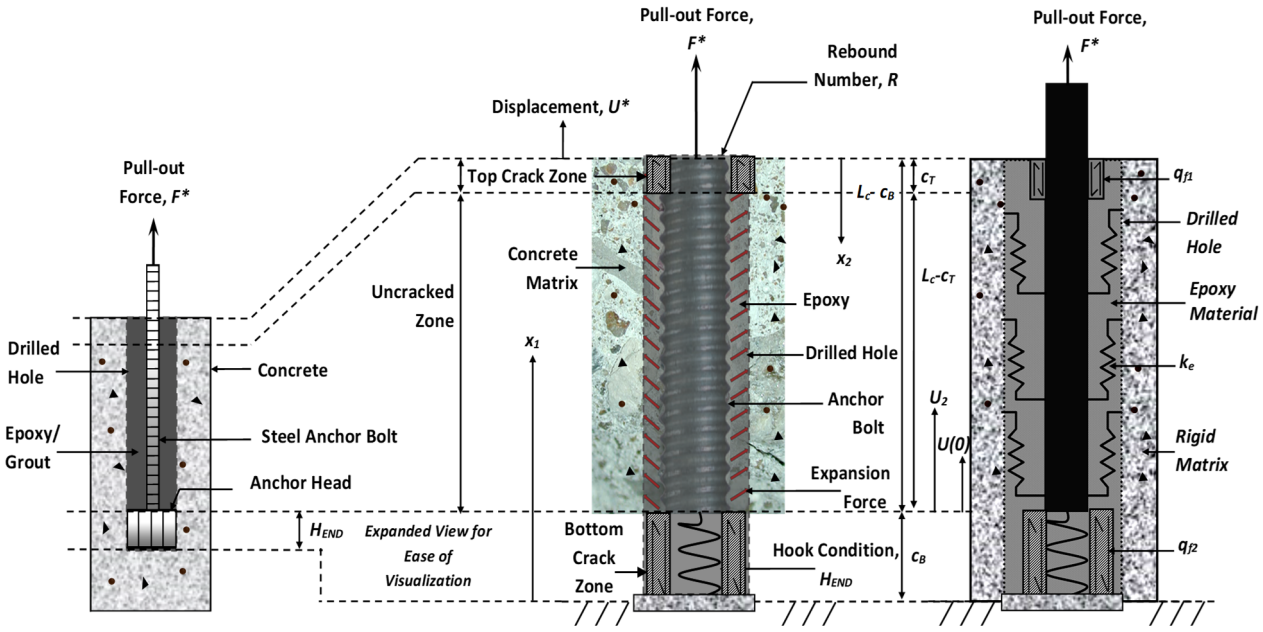

Fig. 3 Schematic visualization of the analytical model for steel anchor bolt embedded in post-drilled hole in concrete installed with epoxy resin

Saleem (2018a), measured the energy imparted by Schmidt hammer's impact on the anchor bolt. It was calculated to be 1.9 joule.

Fig. 2 presents the cumulative energy imparted into the anchor bolt after five rebound impact loadings.

It is brough to the attention of the readers that inducing impact loading on the top of the anchor bolt can lead to internal micro-cracking within the infill epoxy material. This can intern lead to lower bond strength of the anchor bolt. This aspect of the discussion is to highlight to the readers the limitation of the newly proposed non-destructive testing method. Hence, it can be deduced that the newly proposed NDT is limited in application to small and medium anchor bolts. In addition, it can be hypothesized that for anchor bolts with large diameters or long embedment length, the impact energy induced by the traditional Schmidt hammer might not be sufficient to penetrate the entire length of the anchor bolt. Therefore, a new type of rebound device would be needed to test anchor bolts used in rock or slope stabilization, mining industry etc. These topics can be considered as active areas for future research and development. From the past published experimental results (see Saleem *et al*. 2016, Saleem 2017, 2020) it was found that anchor bolts with good bond quality were successfully able to transmit 9 joules of impact energy to the concrete in the near vicinity, thus depicting larger rebound value, R. However, anchor bolts which had lower quality bond or poor quality of concrete depicted lower rebound value, R. This mechanism was used to identify anchor bolts with poor bond quality thus leading to lower to pull-out strength. The present manuscript details the development, validation and material optimization of an analytical model is able to take into consideration material and geometric properties of the anchor bolt. The model is described in the proceeding section.

3. Analytical modeling

Fig. 3 depicts the schematic visualization of the analytical model detailing the steel anchor bolt embedded in the post-construction drilled anchor hole and installed using epoxy resin. The central portion of the diagram presents the visualization of the expansive forces that are generated owing to the pull-out load, F^* applied on the top of the anchor bolt. The portion on the left of the diagram represent the real-world view of the installed anchor bolt, while the view of the right represents the mathematical modeling details, where the epoxy resin material is considered in the model as a shear-lag thus the interfacial cracking happens in shear with the stiffness of k_e. In real-world many kinds of bolts are employed for a large variety of practical applications such as L-shaped end, U-shaped or unheeded straight anchors. The presented analytical model is able to take into consideration the end condition of the anchor using H_{END}, as depicted in Fig. 3. The anchor bolt has a uniform diameter D_B and is assumed to remain elastic during the pull-out loading with the modulus of elasticity as E_A. The concrete surrounding the epoxy resin is modeled as a rigid, except the infill material at the interfacial zone which is treated to non-linear inelastic. Since the diameter of the anchor bolt is much smaller as compared to the embedment length, hence the poisons ratio is neglected. The rationale behind this consideration is that the pull-out displacement of the anchor bolt is much larger as compared to the elongation of the anchor bolt, furthermore, in real-world the anchor bolt elongation results in failure of the anchor bolt before the pull-out extraction is completed which leads to a failed bolt. Hence, the assumption has logical rational background. As shown in Fig. 3 the bond length of the steel anchor bolt has been divided into three distinct portions, the middle portion of the anchor bolt represent the perfect bonded condition without any micro-

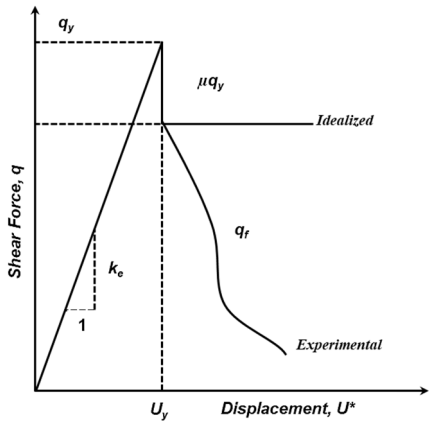

Fig. 4 Constitutive model for epoxy anchor interface

cracking at the interface. However, owing to the impact energy inducted from the impact of Schmidt hammer, two micro-cracks are assumed to have occurred at the top and bottom portion of the anchor bolt. The cracked portions comprise of only the frictional force $q_{fT,B}$. This is because of the interlocking of the anchor bolt ridges and the epoxy resin material. From the point of view of analytical modeling, two possibilities of crack extension are considered i.e., case-1 when only one of the cracks either at the top, c_T or one at the bottom, c_B propagates further owing to the applied external loading. Case-2 is the possibility of both cracks at the top and bottom propagating at the same time. All possibilities arising from the presence of multiple cracks in close proximity are taken into consideration. Evidence provided by (See Kamaya 2003 and Wang *et al*. 1996) for parallel cracks suggest the possibility of crack interaction leading to crack coalescence, crack branching and crack curing. These phenomena are possible because of possibility of stress interaction at the tip of the propagating cracks. Since, crack branching and crack curing are uncontrollable and difficult to predict phenomena, hence these were ignored in the current formulation. Furthermore, the presence of rigid concrete surrounding the epoxy resin eradicates the possibility of crack coalescence. However, combined propagation of both cracks is considered in the presented analytical model. A constant shear force is considered to be the only dominant force in the cracked portion of the interface. Fig. 4 presents the constitutive relationship at the interface of epoxy resin and the anchor bolt. Accordingly, the following constitutive formulations can be expressed

$$F = k_e U(x_1) \qquad 0 < x_1 < (L - c_T) \tag{1}$$

$$F = q_{fT} \qquad (L - c_T) < x_1 < L \tag{2}$$

$$F = k_e U(x_2) \qquad 0 < x_2 < (L - c_B) \tag{3}$$

$$F = q_{fB} \qquad (L - c_B) < x_2 < L \tag{4}$$

$$q_{\tau T} = q_{yT} \tag{5}$$

$$q_{\tau B} = q_{yB} \tag{6}$$

$$a_T = \xi a_B \tag{7}$$

In the above presented constitutive relationships q is the shear force acting at the interface of epoxy infill material and steel anchor bolt. q_{fT}, q_{fB} represent the frictional force present in the cracked portion at the top and bottom cracks as shown in Fig. 3. This frictional force occurs owing to the interlocking of ridges of anchor bolt and the crushed epoxy resin. Where, $q_{\tau T}$, $q_{\tau B}$ and q_{yT}, q_{yB} is the shear stress and yield strength at the top and bottom portion of the interface. While ξ is the crack length controlling factor. The constitutive model of the interface is as depicted in the Fig. 4. The relationship is linear elastic up to the yield point of the material, followed by a sudden drop in strength leading to the frictional force. The sudden crack propagation leads to stress release, which is incorporated into the model as the factor, μ. From experimental evidence of the past (Hariyadi *et al*. 2017, Sugayama *et al*. 2006 and Sumitro and Tsubaki 1998a, b) it is clear that a diminishing frictional force is observed at the anchor-epoxy interface in case of anchor pull-out failure. The crack initially takes the path of least resistance at the interface of epoxy and bolt. This stage is followed by the pulling out of the anchor bolt itself leading to cone type of failure. The proceeding section details the analytical closed form solution for each case of crack extension.

3.1 Modeling for crack propagation when $c_T > c_B$

Let us first take into consideration the case where top crack c_T begins to propagate while the bottom crack is dormant. In this scenario the length of the top crack would increase while the length of the bottom crack would remain the same. The crack growth criterion can be described using the equation provided below

$$\frac{q_{\tau T}}{q_{yT}} > \frac{q_{\tau B}}{q_{yB}} \tag{8}$$

q_y is the yield shear force, depicting the pull-out force, F, the following equilibrium conditions can be written

$$F_x^{"} - q = 0 \tag{9}$$

where, the comma represents the differential operation, $()_{,x}$ with respect to x. Now the constitutive relationship of the steel bolt can be introduced as

$$F = E_C A_C U_x^{"} \tag{10}$$

$$E_C A_C = E_A A_A + \frac{E_I A_I}{K_E} \tag{11}$$

where $E_C A_C$ represents the axial stiffness. The following differential equation for anchor bolt pull-out displacement U can be obtained

$$U_x^{"} - \left(\sqrt{\frac{K_E}{E_A A_A + \frac{E_I A_I}{K_E}}} \right)^2 U = 0 \qquad 0 < x_1 < (L_c - c_T) \tag{12}$$

$$U_x^{"} - \frac{q_{fT}}{E_A A_A + \frac{E_I A_I}{K_E}} = 0 \qquad (L_c - c_T) < x_1 < L_c \tag{13}$$

Now, $\mathcal{Y}$ is defined as

$$\mathcal{Y} = \sqrt{\frac{K_E}{E_A A_A + \frac{E_I A_I}{K_E}}} \tag{14}$$

Now stating that F^* is the pull-out force when $x_T = L_C$, the boundary and the continuity conditions can be expressed as below

$$H_{END} U(0) = N(0) \tag{15}$$

$$E_C A_C U_x^{"}(L_c) = F^* \tag{16}$$

$$U(L_c - c_T)^- = U(L_c - c_T)^+ \tag{17}$$

$$U_x^{"}(L_c - c_T)^- = U_x^{"}(L_c - c_T)^+ \tag{18}$$

By applying the above developed formulations, the following analytical solution can be reached related to anchor bolt pull-out deformation

$$U(x) = \frac{P^* - q_{fT} c_T}{E_A A_A + \frac{E_I A_I}{K_E} \mathcal{Y}} \left(\frac{cosh(\mathcal{Y} x_T)}{\mathfrak{Y}_1} + \frac{sinh(\mathcal{Y} x_T)}{\mathfrak{Y}_2} \right) \qquad 0 < x_1 < (L_c - a_T) \tag{19}$$

$$U(x) = \frac{q_{fT} c_T^2}{2 E_C A_C} + \frac{F^* - q_{fT} L_c}{E_C A_C} x_1 - \frac{q_{fT} (L_c - c_T)^2}{2 E_C A_C} + \frac{F^* - q_{fT} x_1}{E_C A_C \mathcal{Y}} (\mathfrak{Y}_3) - \frac{F^* - q_{fT} L_c}{E_C A_C} (L_c - c_T) \qquad (L_c - c_T) < x_1 < L_c \tag{20}$$

$$\mathfrak{Y}_1 = \frac{H_{END}}{E_A A_A + \frac{E_I A_I}{K_E} \mathcal{Y}} cosh\, \mathcal{Y} (2L_c - c_T) + sinh\, \mathcal{Y} (2L_c - c_T) \tag{21}$$

$$\mathfrak{Y}_2 = cosh\, \mathcal{Y} (2L_c - c_T) + \frac{E_A A_A + \frac{E_I A_I}{K_E} \mathcal{Y}}{H_{END}} sinh\, \mathcal{Y} (2L_c - c_T) \tag{22}$$

$$\mathfrak{Y}_3 = \frac{cosh\, \mathcal{Y} (2L_c - c_T)}{\mathfrak{Y}_1} + \frac{sinh\, \mathcal{Y} (2L_c - c_T)}{\mathfrak{Y}_2} \tag{23}$$

Now the total anchor bolt pull-out displacement can be calcualted using the following equation

$$U^* = \frac{P^* - q_{fT} c_T}{E_A A_A + \frac{E_I A_I}{K_E} \mathcal{Y}} \mathfrak{Y}_3 + \frac{P^* - \frac{1}{2} q_{fT} c_T}{E_A A_A + \frac{E_I A_I}{K_E}} c_T \tag{24}$$

Crack growth occurs when the applied shear force reaches the yield value, afterwards the shear force at the cracked interface of the epoxy material and the anchor bolt is assumed to be equal to the frictional shear force, q_f.

$$q_{fI} = \mu\, q_{yI} \tag{25}$$

$$\mu = \mu_o \qquad 0 \le \mu_o \le 1 \tag{26}$$

The coefficient μ represents the stress release that occurs after the crack growth and is as shown in Fig. 4. Now for the case when cracking occurs, $q = q_{yI}$ at $x = L_c - c_T$, Now Force, F^* can be calculated as

$$F^* = q_{fT} c_T + \frac{q_{yT}}{\mathcal{Y}} \left\{ \frac{\mathfrak{Y}_1 \mathfrak{Y}_2}{\mathfrak{Y}_4} \right\} \tag{27}$$

$$\mathfrak{Y}_4 = \mathfrak{Y}_1\, sinh\, \mathcal{Y} (L_c - c_T) + \mathfrak{Y}_2\, cosh\, \mathcal{Y} (L_c - c_T) \tag{28}$$

The force at which the crack at the top of the anchor bolt starts to propagate downwards can be calculated using the Eqs. (24) and (27). The final peak displacement of the anchor bolt can be calculated using the Eq. (24). On the cracked portion of the infill epoxy material only the frictional forces exists because of interlocking of bolt ridges and epoxy resin. Since the elongation of the anchor bolt is negligible as compared to the anchor bolt pull-out displacement, hence, it is ignored in the presented formulation. Once the cracking is initiated it propagates along the weakest path with is considered to the ITZ (see Sumitro and Tsubaki 1998a, b) till complete failure occurs. After complete cracking, the anchor bolt is pulled out of concrete. The above presented equations are used for experimental validation in the proceeding section.

3.2 Modeling for crack propagation when $c_B > c_T$

The second possibility of crack propagation can be the case when crack the bottom, c_B, start to extend, while the crack at top, c_T, remains dormant. Under such condition the length of the bottom crack, c_B, will increase till it reaches to the top of the anchor bolt. The crack propagation criterion for this case, when $c_B > c_T$ can be written as

$$\frac{q_{\tau T}}{q_{yT}} < \frac{q_{\tau B}}{q_{yB}} \tag{29}$$

Then the equilibrium condition is similar to the one presented in Eqs. (9) to (11). Thus, the anchor bolt pull-out displacement differential equations can be written as

$$U_x^{"} - \left(\sqrt{\frac{K_E}{E_A A_A + \frac{E_I A_I}{K_E}}} \right)^2 U = 0 \qquad 0 < x_2 < (L_c - c_B) \tag{30}$$

$$U_x^{"} - \frac{q_{fT}}{E_A A_A + \frac{E_I A_I}{K_E}} = 0 \qquad (L_c - c_B) < x_2 < L_c \tag{31}$$

Now, $\mathcal{Y}$ is defined as

$$\mathcal{Y} = \sqrt{\frac{K_E}{E_A A_A + \frac{E_I A_I}{K_E}}} \tag{32}$$

Now stating that F^* is the pull-out force when $x_B = L_C$,

the boundary and the continuity conditions can be expressed as below

$$H_{END}U(0) = N(0) \tag{33}$$

$$E_C A_C U_x^{"}(L) = F^* \tag{34}$$

$$U(L_c - c_B)^- = U(L_c - c_B)^+ \tag{35}$$

$$U_x^{"}(L_c - c_B)^- = U_x^{"}(L_c - c_B)^+ \tag{36}$$

By applying the above developed formulations, the following analytical solution can be reached related to anchor bolt pull-out deformation

$$U(x) = \frac{P^* - q_{fB}c_B}{E_A A_A + \frac{E_I A_I}{K_E}\text{Ч}}\left(\frac{cosh(\text{Ч}x_B)}{\text{Þ}_1^{"}} + \frac{sinh(\text{Ч}x_B)}{\text{Þ}_2^{"}}\right) \tag{37}$$

$$\begin{aligned} U(x) = {} & \frac{q_{fB}c_B^2}{2E_C A_C} + \frac{F^* - q_{fB}L_c}{E_C A_C}x_2 - \frac{q_{fB}(L_c - c_B)^2}{2E_C A_C} \\ & + \frac{F^* - q_{fB}x_2}{E_C A_C \text{Ч}}(\text{Þ}_3^{"}) - \frac{F^* - q_{fB}L_c}{E_C A_C}(L_c - c_B) \\ & (L_c - c_B) < x_2 < L_c \end{aligned} \tag{38}$$

$$\begin{aligned} \text{Þ}_1^{"} = {} & \frac{H_{END}}{E_A A_A + \frac{E_I A_I}{K_E}\text{Ч}} cosh\,\text{Ч}\,(2L_c - c_B) \\ & + sinh\,\text{Ч}\,(2L_c - c_B) \end{aligned} \tag{39}$$

$$\begin{aligned} \text{Þ}_2^{"} = {} & cosh\,\text{Ч}\,(2L_c - c_B) \\ & + \frac{E_A A_A + \frac{E_I A_I}{K_E}\text{Ч}}{H_{END}} sinh\,\text{Ч}\,(2L_c - c_B) \end{aligned} \tag{40}$$

$$\text{Þ}_3^{"} = \frac{cosh\,\text{Ч}\,(2L_c - c_B)}{\text{Þ}_1^{"}} + \frac{sinh\,\text{Ч}\,(2L_c - c_B)}{\text{Þ}_2^{"}} \tag{41}$$

Now the total anchor bolt pull-out displacement can be calcualted using the following equation

$$U^* = \frac{P^* - q_{fB}c_B}{E_A A_A + \frac{E_I A_I}{K_E}\text{Ч}}\text{Þ}_3^{"} + \frac{P^* - \frac{1}{2}q_{fB}c_B}{E_A A_A + \frac{E_I A_I}{K_E}}c_B \tag{42}$$

Now for the case when cracking occurs, $q = q_{yI}$ at $x = L_c - c_B$, Now Force, F^* can be calculated as

$$F^* = q_{fB}c_B + \frac{q_{yT}}{\text{Ч}}\left\{\frac{\text{Þ}_1^{"}\text{Þ}_2^{"}}{\text{Þ}_4^{"}}\right\} \tag{43}$$

$$\text{Þ}_4^{"} = \text{Þ}_1^{"} sinh\,\text{Ч}\,(L_c - c_B) + \text{Þ}_2^{"} cosh\,\text{Ч}\,(L_c - c_B) \tag{44}$$

The force at which the crack at the bottom of the anchor bolt starts to propagate upwards can be calculated using the Eqs. (42) and (44). The final peak displacement of the bolt can be calculated using the Eq. (42).

3.3 Modeling for crack propagation when $c_B = c_T$

The third case taken into consideration is the rare event when both top and bottom cracks start to propagate simultaneously towards each other. As mentioned in the earlier section that all possibilities pertaining to crack interaction owing to the presence of multiple cracks in close vicinity were taken into consideration such as crack curving, crack branching and crack coalescence. However, in light of the geometry of the presented problem and evidence provided in the literature the crack interaction was ruled out. However, a rare chance of both cracks propagating instantaneously still pertains. Hence, the analytical formulation related to this situation when $c_B = c_T$ is presented. The crack extension criterion for the case when $c_B = c_T$ can be stipulated as

$$\frac{q_{\tau T}}{q_{yT}} = \frac{q_{\tau B}}{q_{yB}} \tag{45}$$

Then the equilibrium condition is similar to the one presented in Eqs. (9) to (11). Thus, the anchor bolt pull-out displacement differential equations can be written as

$$\begin{aligned} & U_x^{"} - \left(\sqrt{\frac{K_E}{E_A A_A + \frac{E_I A_I}{K_E}}}\right)^2 U = 0 \\ & 0 < x < (L_c - (c_T + c_B)) \end{aligned} \tag{46}$$

$$\begin{aligned} & U_x^{"} - \frac{q_{favg}}{E_A A_A + \frac{E_I A_I}{K_E}} = 0 \\ & \left(L_c - (c_T + c_B)\right) < x < L_c \end{aligned} \tag{47}$$

Now, Ч is defined as

$$\text{Ч} = \sqrt{\frac{K_E}{E_A A_A + \frac{E_I A_I}{K_E}}} \tag{48}$$

Now stating that F^* is the pull-out force when $x_T = x_B = L_C$, the boundary and the continuity conditions can be expressed as below

$$H_{END}U(0) = N(0) \tag{49}$$

$$E_C A_C U_x^{"}(L) = F^* \tag{50}$$

$$U(L_c - c_T)^- = U(L_c - c_T)^+ \tag{51}$$

$$U_x^{"}(L_c - c_T)^- = U_x^{"}(L_c - c_T)^+ \tag{52}$$

$$U(L_c - c_B)^- = U(L_c - c_B)^+ \tag{53}$$

$$U_x^{"}(L_c - c_B)^- = U_x^{"}(L_c - c_B)^+ \tag{54}$$

By applying the above developed formulations, the following analytical solution can be reached related to anchor bolt pull-out deformation

$$U(x) = \frac{P^* - \left(q_{fT}c_T + q_{fB}c_B\right)}{E_A A_A + \frac{E_I A_I}{K_E}\text{Ч}}\left(\frac{cosh(\text{Ч}x)}{\text{Ъ}''_{1\prime}} + \frac{sinh(\text{Ч}x)}{\text{Ъ}''_{2\prime}}\right) \quad 0 < x < \left(L_c - (c_T + c_B)\right) < x < L_c \tag{55}$$

$$U(x) = \frac{q_{fT}c_T^2 + q_{fB}c_B^2}{2E_C A_C} + \frac{F^* - \left(q_{fT} + q_{fB}\right)L_c}{E_C A_C}x - \frac{q_{fT}(L_c - c_T)^2 + q_{fB}(L_c - c_B)^2}{2E_C A_C} + \frac{F^* - \left(q_{fT}x_1 + q_{fB}x_2\right)}{E_C A_C \text{Ч}}\left(\text{Ъ}''_{3\prime}\right) - \frac{F^* - q_{favg}L_c}{E_C A_C}\left(L_c - (c_T + c_B)\right) \tag{56}$$

$$\text{Ъ}''_{1\prime} = \frac{K_{END}}{E_T A_T \Gamma} cosh\,\text{Ч}\left(2L_c - (c_T + c_B)\right) + sinh\,\text{Ч}\left(2L_c - (c_T + c_B)\right) \tag{57}$$

$$\text{Ъ}''_{2\prime} = cosh\,\text{Ч}\left(2L_c - (c_T + c_B)\right) + \frac{E_T A_T \Gamma}{K_{END}} sinh\,\text{Ч}\left(2L_c - (c_T + c_B)\right) \tag{58}$$

$$\text{Ъ}''_{3\prime} = \frac{cosh\,\text{Ч}\left(2L_c - (c_T + c_B)\right)}{\text{Ъ}''_{1\prime}} + \frac{sinh\,\text{Ч}\,(2L_c - (c_T + c_B))}{\text{Ъ}''_{2\prime}} \tag{59}$$

Now the pull-out displacement of the bolt can be calculated by the below equation

$$U^* = \frac{P^* - \left(q_{fT}c_T + q_{fB}c_B\right)}{E_A A_A + \frac{E_I A_I}{K_E}\text{Ч}}\text{Ъ}''_{3\prime} + \frac{P^* - \frac{1}{2}\left(q_{fT}c_T + q_{fB}c_B\right)}{E_A A_A + \frac{E_I A_I}{K_E}}(c_T + c_B) \tag{60}$$

Now for the case when cracking occurs, $q = q_{yI}$ at $x = L_c - (c_T + c_B)$, Now Force, F^* can be calculated as

$$F^* = q_{favg}(c_T + c_B) + \frac{q_{yI}}{\text{Ч}}\left\{\frac{\text{Ъ}''_{1\prime}\text{Ъ}''_{2\prime}}{\text{Ъ}''_{4\prime}}\right\} \tag{61}$$

$$\text{Ъ}''_{4\prime} = \text{Ъ}''_{1\prime}\,sinh\,\text{Ч}\left(L_c - (c_T + c_B)\right) + \text{Ъ}''_{2\prime}\,cosh\,\text{Ч}\,(L_c - (c_T + c_B)) \tag{62}$$

The force at which the crack at the bottom of the anchor bolt starts to propagate upwards can be calculated using the Eqs. (54) and (56). The final peak displacement of the anchor bolt can be calculated using the Eq. (54).

4. Calculation algorithm

Fig. 5 represents the conceptual representation of the calculation algorithm developed for conducting the analytical calculations. MATLAB was used for model simulations. As presented in the Fig. 5 the calculation algorithm starts with the defining of relevant geometric and material parameter. These parameters are related to the epoxy infill, shape and size of the anchor bolt, the end condition of the anchor i.e., U-shaped hook, L-shaped hook or straight anchors. This allows the research team to simulate the deformational response for a variety of anchors. Afterwards, the past loading history of the anchor-infill is evaluated, this stage allows for inclusion of any prior loading or defects encountered at the anchor installation stage. Upon addition of relevant parameters, the crack propagation criterion is evaluated for top crack, bottom crack or simultaneous crack propagation. Upon satisfying any one of the three cases related to crack development, the new value of anchor bolt displacement and loading are calculated for the new growth in crack length. This cycle is repeated till the entire infill interface is cracked, afterwards the anchor bolt is subjected to only frictional forces along its embedment length with subsequent pull-out from the embedded epoxy infill.

Prior to the application of force, the entire infill interface is in bonded state, however, as the applied force increases and the stress q_I reaches the yield limit, q_{yI}, the crack is initiated either at the top or at the base of the epoxy interface. Since, the crack travels along the path of minimum resistance, hence the assumption that the crack will travel along the interface is valid. Upon further increase in the applied external loading, the crack growth continues till it reaches the base of the anchor bolt. At this stage a sudden drop in the pull-out load is observed, followed by

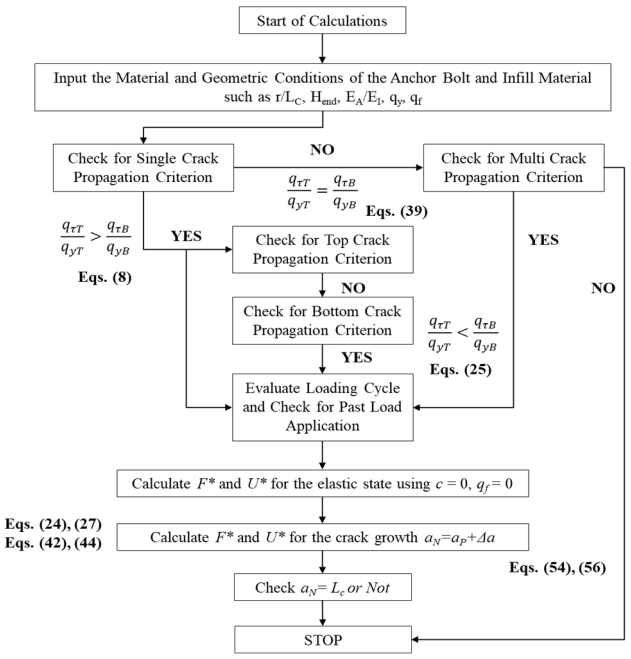

Fig. 5 Conceptual calculation algorithm

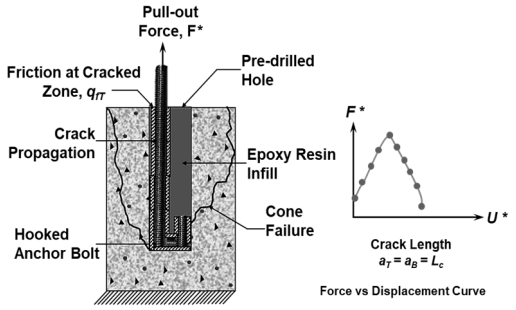

Fig. 6 Conceptual schematic depiction of deformational response for straight anchors

by the extraction of the anchor bolt from the pre-drilled hole. The force F^* can be calculated using $F^* = q_{fl}(L_c - U^*)(cL_c - U)/(cL_c - U^*)$ (see Sumitro and Tsubaki 1998) and the complete displacement of steel bolt can be calculated as $U = cL_c$. It is to be highlighted for the readers that the tensile stress of the bolt is checked after each loading cycle, in case the tensile stress reaches the yield value of the steel, rupture of anchor is assumed to have occurred.

Sumitro and Tsubaki (1998a, b), Saleem *et al*. (2016) and Saleem (2017) tested a variety of anchor bolts and fibers embedded in concrete. Through their experimentations, it was evident that the end type of the bolt has a profound effect on its deformational response. Bolts with hooked ends depicted higher load carrying capacity with failed in cone type of failure as shown in Fig. 6, while the anchor bolts with straight end depicted large displacement following the interfacial cracking and could be extracted as a whole from the embedded epoxy resin as shown in Fig. 7.

5. Optimum epoxy infill properties

Material properties of the infill epoxy/grout resin play an important role in ensuring that the anchor bolt is able to achieve the desired designed load carrying strength.

$$T = O_1 f_1 + O_2 f_2 \tag{63}$$

$$f_1 = \frac{U^*}{U^*_{max}} \tag{64}$$

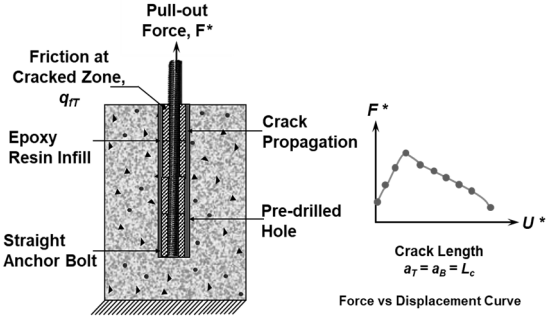

Fig. 7 Conceptual schematic depiction of deformational response for bent anchors

$$f_2 = \frac{D}{D_{max}} \tag{65}$$

In this regard, the aim of the researcher group was to provide insight into the optimum epoxy infill material properties that lead to optimum failure of the anchor bolt. Optimum failure of the anchor bolt is defined as the failure condition which leads to minimum damage to the surrounding concrete corresponding to smallest pull-out displacement. The combination of the material properties that provide the optimum failure are declared to be the optimized material properties. The in-depth analysis of the presented analytical model reveals that the elastic modulus of the infill material should be kept high in order to control the peak displacement of the anchor bolt, while the shear strength should be kept in the range close to the yield strength of steel bolt so that the maximum pull-out strength can be achieved without causing the anchor bolt to rupture or buckle under yielding. These conditions have been defined in the form of a target function; T as presented in Eqs. (57) to (59). Where O_1 and O_2 are the weightage constants representing the importance of each parameter investigated in the presented manuscript. These have a value of each equal to 0.5. f_1, f_2 are the normalized displacements of the anchor bolt and the damage caused to the surrounding concrete. The target optimum function is defined as the set of properties for the infill epoxy material that leads to the lowest value of target function, T.

To achieve the desired target function, various combinations of material input properties were investigated to achieve the target of reduced pull-out displacement at maximum pull-out strength without causing yielding into the anchor bolt. Table 1 presents the various combinations of parameters investigated; each combination is depicted using a parameter number. Fig. 8 presents the target function with regards to parameter set number for 10 combinations. The values of f_1 and f_2 are obtained by a combination of parameters. From the presented figure it is evident that as the shear strength of the infill material is increased along with reducing the elastic modulus, the resulting target function yields the minimum value. From the presented result, it can be seen that peak-optimum value of the infill materials lies somewhere between parameter 2 to 3 which corresponds to E_I/E_A of 0.2 to 0.3 and the shear strength ratio of 0.90 to 0.85. At this value the target function yielded the lowest value.

In light of the presented analysis further detailed parametric evaluation was conducted to pinpoint the exact combination of parameters that yields optimum failure of the anchor bolts. All possible combinations of infill epoxy parameters in the range of E_I/E_A of 0.2 to 0.3 and q_{yI}/ q_{yA} of 0.85 to 0.90 were tested and results were analyzed. This analysis yielded the minimum value of target function, T at 0.293. A comparison of the peak pull-out load and displacement yielded by the optimum epoxy infill material properties was conducted with the worst possible combination of parameters shown at combination number 10. From the analysis it was evaluated that the optimum combination of epoxy infill material properties was able to lower the peak pull-out displacement by 26% and the

Table 1 Parametric groups and target function

Para. set. no.	$\frac{E_I}{E_A}$	$\frac{q_{yI}}{q_{yA}}$	f_1	f_2	T
1	0.10	0.95	0.831	0.091	0.369
2	0.20	0.90	0.611	0.055	0.343
3	0.30	0.85	0.607	0.079	0.317
4	0.40	0.80	0.622	0.088	0.433
5	0.50	0.75	0.681	0.089	0.412
6	0.60	0.70	0.777	0.117	0.445
7	0.70	0.65	0.931	0.298	0.498
8	0.80	0.60	0.949	0.334	0.573
9	0.85	0.55	0.971	0.588	0.694
10	0.90	0.50	1.000	1.000	1.000

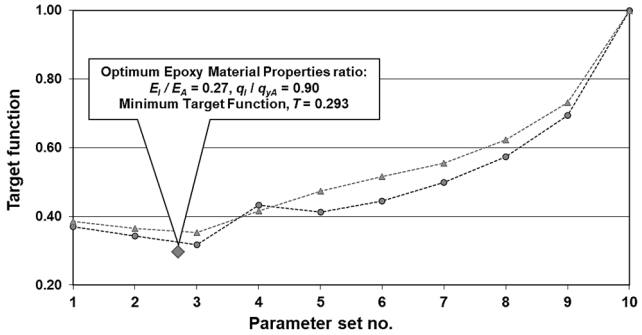

Fig. 8 Target function with respect to parametric set number

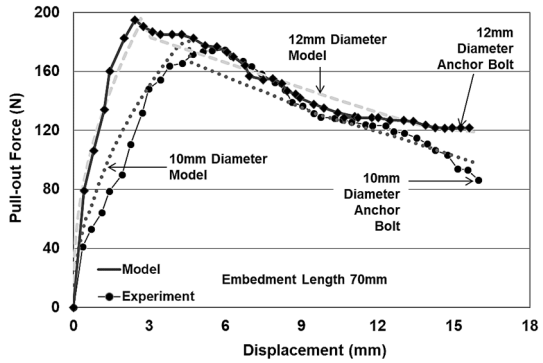

Fig. 9 Experimental versus analytical model simulation Pull-out deformational response for 10 mm and 12 mm diameter anchor bolt with embedment length of 70 mm

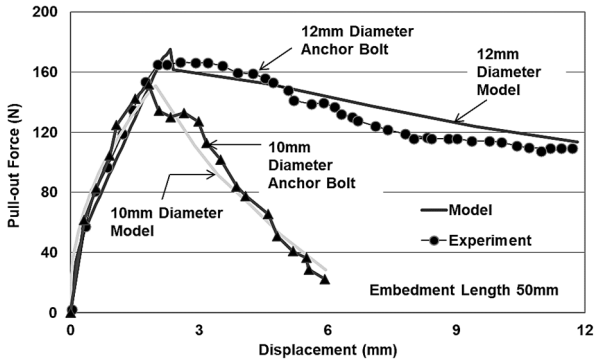

Fig. 10 Experimental versus analytical model simulation Pull-out deformational response for 10 mm and 12 mm diameter anchor bolt with embedment length of 50 mm

damage caused to the concrete adjacent to the anchor bolt hole reduced by 93%. Hence, from the above presented results and discussion it can be deduced that the optimum epoxy infill material properties can lead to the desired controlled pull-out failure of post-installed anchor bolts.

6. Experimental validation

The reliability of the presented model was evaluated by comparing its predicted load-displacement curve to the experimental results. For this purpose, the pull-out deformational response for 10 mm and 12 mm diameter stainless steel anchor bolts embedded 50 mm and 70 mm into the concrete were used for comparison (See Sugiyama *et al*. 2006 and Hariyadi *et al*. 2017). Figs. 9 and 10 represent the comparison between the analytical model and experimental results. The horizontal axis presents displacements in mm while the vertical axis presents the pull-out force, F^* in N. The yield strength of the anchor bolts was 575 MPa and the ultimate strength was 780 MPa. The anchor bolt radius to embedment depth ratio was 0.1 and 0.12 respectively. The elastic modulus of the bolt, E_A was taken as 2.1×10^5 N/mm^2 while the shear stiffness of the epoxy infill was taken as $k = 0.2 \times 10^5$ N/mm^2 (Sumitro and Tsubaki 1998a). The end state of the anchor bolt, H_{END} has a profound impact on the deformational response of the anchor bolt. For straight anchor bolts presented in the current manuscript for experimental validation, this value can be considered negligible. However, for other types of bent or hooked anchors this value should be calculated through experimentation. This aspect can be considered as an active area for future research and development.

From Figs. 9 and 10 it can be seen that before the application of the loading, there is no deformations in the anchor bolt. Upon increase in applied loading the infill epoxy materials remains in elastic range. Further increase in loading causes the weakest path for crack propagation i.e., interface to crack. This results in displacement of the anchor bolt. This phenomenon continues till the entire length of the anchor bolt epoxy interface is cracked, after which a sudden drop in pull-out load occurs. This can be attributed to stress release phenomenon owing to crack development. From this point onwards the entire anchor epoxy interface is only comprised of friction shear force, the load displacement curve begins to descend rapidly owing to the loss of rib force followed by the cone failure. The pull-out force F^* can be calculate using $F^* = q_{fI}(L_c - U^*)(cL_c - U)/(cL_c - U^*)$ (see Sumitro and Tsubaki 1998) and the complete displacement of steel bolt can be calculated as $U = cL_c$ at this point the bolt is fully pulled-out.

From the presented results, it can be seen that a good agreement exists between the presented analytical model and the experimental results. Hence, it can be deduced with

confident that the presented anchor pull-out model is able to predict the load-displacement response of a variety of steel bolts. Furthermore, the average gap between the analytical model and the experimental peak load carrying capacity of the anchor bolt was 2.6%, which adds confidence to the reliability of the presented model.

7. Conclusions

A pull-out deformational response prediction model is presented which is capable of taking into consideration micro-cracking owing to the impact loading induced by the Schmidt hammer at the anchor epoxy interface. From the provided results and discussion, the following conclusions can be drawn.

(1) The presented analytical model is successful in taking into consideration the material and geometric properties of the anchor bolt and epoxy resin along with taking into account the effects of various type of end conditions of the deformational response of anchor bolt.
(2) Material optimization analysis resulted in a set of optimum properties that were able to reduce the peak pull-out displacement by 26% and the lower the damage to the surrounding concrete by 93%.
(3) The model was able to show good agreement in comparison of the simulation results of the deformational response to the experimental evidence of anchor bolt pull-out testing.

Acknowledgments

The author is grateful to the Deanship of Scientific Research (DSR) at Imam Abdulrahman Bin Faisal University, Kingdom of Saudi Arabia for the continued support and guidance. The publication is part of the project funded by the DSR-IAU under the project ID: 2020-158-ENG.

References

ACI 349-13 (2013), Code requirements for nuclear safety related concrete structures, American Concrete Institute, USA.

ACI 318-14 (2014), Building Code requirements for structural concrete and commentary, American Concrete Institute, USA.

Barani, O.R. and Khoei, A.R. (2014), "3D modeling of cohesive crack growth in partially saturated porous media: A parametric study", *Eng. Fract. Mech.*, **124-125**, 272-286. https://doi.org/10.1016/j.engfracmech.2014.04.016

Caggiano, A. and Martinelli, E. (2012), "A unified formulation for simulating the bond behavior of fibers in cementitious materials", *Mater. Des.*, **42**, 204-213. https://doi.org/10.1016/j.matdes.2012.05.003

Ceci, A.M., Casas, J.R. and Ghosn, M. (2012), "Statistical analysis of existing models for flexural strengthening of concrete bridge beams under FRP sheets", *Construct. Build. Mater.*, **27**, 490-520. https://doi.org/10.1016/j.conbuildmat.2011.07.014

Chen, Y. (2014), "Experimental study and stress analysis of rock bolt anchorage performance", *J. Rock Mech. Geotech. Eng.*, **6**, 428-437. https://doi.org/10.1016/j.jrmge.2014.06.002

Eligehausen, R. and Balogh, T. (1995), "Behavior of fasteners loaded in tension in cracked reinforced concrete", *ACI Struct. J.*, **92**(3), 365-379.

Eligehausen, R., Mallee, R. and Silva, J.F. (2006), *Anchorage in Concrete Construction*, WILEY Publications. ISBN: 978-3-433-01143-0

Guillet, T. (2011), "Behavior of metal anchors under combined tension and shear cycling loads", *ACI Struct. J.*, **108**(3), 315-323.

Hariyadi, Munemoto, S. and Sonoda, Y. (2017), "Experimental analysis of anchor bolt in concrete under the pull-out loading", *Sustain. Civil Eng. Struct. Constr. Mater.*, *SCESCM*, **171**, 926-933. https://doi.org/10.1016/j.proeng.2017.01.391

Hoehler, M.S. and Eligehausen, R. (2008a), "Behavior and testing of anchors in simulated seismic cracks", *ACI Struct. J.*, **105**(3), 348-357.

Hoehler, M.S. and Eligehausen, R. (2008b), "Behavior of anchors in cracked concrete under tension cycling at near-ultimate loads", *ACI Struct. J.*, **105**(5), 601-608.

Kamaya, M. (2003), "A crack growth evaluation method for interacting multiple cracks", *JSME Int. J.*, **46**(1), 15-23. https://doi.org/10.1299/jsmea.46.15

Lê Minh, B., Maitournam, M.H. and Doquet, V. (2012), "A cyclic stead-state method for fatigue crack propagation: evaluation of plasticity-induced crack closure in 3D", *Int. J. Solids Struct.*, **49**, 2301-2313. https://doi.org/10.1016/j.ijsolstr.2012.04.040

Mallee, R., Eligehausen, R., Fuchs, W., Bergmeister, K., Fingerloos, F. and Worner, J.D. (2013), *Design of fastenings for use in concrete*: *The CEN/TS 1992-4 Provisions*, WILEY Publications. ISBN: 978-3-433-03044-8

Munemoto, S. and Sonoda, Y. (2017), "Experimental analysis of anchor bolt in concrete under the pull-out loading", *Procedia Eng.*, **171**, 926-933. https://doi.org/10.1016/j.proeng.2017.01.391

Ouyang, C., Pacios, A. and Shah, S.P. (1994), "Pull-out of inclined fibers from cementitious matrix", *J. Eng. Mech.*, **120**(12), 2641-2659. https://doi.org/10.1061/(ASCE)0733-9399(1994)120:12(2641)

Philipp, M., Eligehausen, R., Hutchinson, T.C. and Matthew, S.H. (2016), "Behavior of post-installed anchors tested by stepwise increasing cyclic load protocols", *ACI Struct. J.*, **113**(5), 997-1008. https://doi.org/10.14359/51689023

Saleem, M. (2017), "Study to detect bond degradation in reinforced concrete beams using ultrasonic pulse velocity test method", *Struct. Eng. Mech., Int. J.*, **64**(4), 427-436. https://doi.org/10.12989/sem.2017.64.4.427

Saleem, M. (2018a), "Evaluating the pull-out load capacity of steel bolt using Schmidt hammer and ultrasonic pulse velocity test", *Struct. Eng. Mech., Int. J.*, **65**(5), 601-609. https://doi.org/10.12989/sem.2018.65.5.601

Saleem, M. (2018b), "Multiple crack extension model of steel anchor bolts subjected to impact loading", *Constr. Build. Mater.*, **180**, 364-374. https://doi.org/10.1016/j.conbuildmat.2018.05.275

Saleem, M. (2018c), "Cyclic shear-lag model of steel bolt for concrete subjected to impact loading", *J. Mater. Civil Eng.*, **30**(3), 1-9. https://doi.org/10.1061/(ASCE)MT.1943-5533.0002204

Saleem, M. (2020), "Assessing the load carrying capacity of concrete anchor bolts using non-destructive tests and artificial multilayer neural network", *J. Build. Eng.*, **30**, 1-13. https://doi.org/10.1016/j.jobe.2020.101260

Saleem, M. and Almakhayitah, A.M. (2020), "Development of non- destructive testing method to evaluate the bond quality of reinforced concrete beam", *Struct. Eng. Mech., Int. J.*, **74**(3), 313-323. https://doi.org/10.12989/sem.2020.74.13.313

Saleem, M. and Hector, G. (2021), "Using artificial neural network and non-destructive test for crack detection in concrete surrounding the embedded steel reinforcement", *Struct. Concrete*, **1**, 1-19. https://doi.org/10.1002/suco.202000767

Saleem, M. and Hosoda, A. (2021), "Latin hypercube sensitivity analysis and non-destructive test to evaluate the pull-out strength of steel anchor bolts embedded in concrete", *Constr. Build. Mater.*, **290**, 123256. https://doi.org/10.1016/j.conbuildmat.2021.123256

Saleem, M. and Nasir, M. (2016), "Bond evaluation of steel bolts for concrete subjected to impact loading", *J. Mater. Struct.*, **49**(9), 3635-3646. https://doi.org/10.1617/s11527-015-0745-9

Saleem, M., Al-Kutti, W., Al-Akhras, N. and Haider, H. (2016), "Non-destructive Testing Method to Evaluate the Load Carrying Capacity of Concrete Anchors", *J. Constr. Eng. Manag.*, **142**(5), 17-29. https://doi.org/10.1061/(ASCE)CO.1943-7862.0001105

Sugiyama, N., Tsubaki, T. and Hayashi, K. (2006), "Pull-out model of anchor bars of flexural members under reversed cyclic loading", *Proceedings of the Japan Concrete Institute*, **28**(2), 1117-1122.

Sumitro, S. and Tsubaki, T. (1998a), "Micromechanical fiber pull-out model for steel fiber reinforced concrete", *Doboku Gakkai Ronbunshu*, **40**(599), 155-163. https://doi.org/10.2208/jscej.1998.599_155

Sumitro, S. and Tsubaki, T. (1998b), "Microstructural pullout model of steel fiber reinforced concrete", *Proceedings of FRAMCOS-3, Fracture Mechanics of Concrete Structures*, AEDIFICATIO Publishers, Germany, Vol. I, pp. 521-530.

Takiguchi, K., Harada, R. and Ishizeki, K. (1999), "Pull out strength of an anchor bolt embedded in cracked concrete", *Transactions of the 15th international conference on structural mechanics in reactor technology* (*SMiRT-15*), pp. 305-310.

Wang, Y.Z., Atkinson, J.D., Akid, R. and Parkins, R.N. (1996), "Crack Interaction, Coalescence and Mixed Mode Fracture Mechanics", *Fatigue Fract. Eng. Mater. Struct.*, **19**(1), 51-63.

Yang, K.H. and Ashour, A.F. (2009), "Mechanism analysis for concrete breakout capacity of single anchors in tension", *ACI Struct. J.*, **105**(5), 73-94.

Zamora, N.A., Cook, R.A., Konz, R.C. and Consolazio, G.R. (2003), "Behavior and design of single, headed and unheaded, grouted anchors under tensile load", *ACI Struct. J.*, **100**(2), 222-230.

CC

Notations

A_B = area of anchor bolt
c_T, c_B = cracked portion at the top and bottom
μ = stress reduction ratio, q_f/q_y
D_B = bolt diameter
E_A = elastic modulus of anchor bolt
E_I = elastic modulus of epoxy at interface
k_E = shear stiffness of interface
H_{END} = Bolt hook condition
NDT = Non-destructive test
L_C = Complete length of steel anchor bolt
L_O = anchor bolt outside the hole length
L_E = anchor bolt embedment length
U = anchor bolt pull-out displacement
D = Damage to surrounding concrete
O = importance factor
L_E = anchor bolt embedment length
q_T, q_B = shear force per unit length at interface of epoxy and anchor for top and bottom zones
q_{fT}, q_{fB} = frictional force per unit length at the top and bottom cracked zone of the anchor-epoxy interface
q_{favg} = average frictional force per unit length
q_{yT}, q_{yB} = maximum shear force per unit length at the top and bottom zone
$q_{\tau T}$, $q_{\tau B}$ = maximum stress at the top and bottom interface zone
ξ = crack control factor
q = interface parameter for infill epoxy and bolt
$\mathcal{D}$", $\mathcal{D}_{1,2,3}$ = interface parameter
R = Schmidt hammer rebound number